Initial- and Processive-Cut Products Reveal Cellobiohydrolase Rate Limitations and the Role of Companion Enzymes

Jerome M. Fox,[†,‡] Seth E. Levine,[†,‡] Douglas S. Clark,*,[‡] and Harvey W. Blanch*,[‡]

[†]Energy Biosciences Institute and [‡]Department of Chemical and Biomolecular Engineering, University of California, Berkeley, California 94720, United States

Ⓢ *Supporting Information*

ABSTRACT: Efforts to improve the activity of cellulases, which catalyze the hydrolysis of insoluble cellulose, have been hindered by uncertainty surrounding the mechanistic origins of rate-limiting phenomena and by an incomplete understanding of complementary enzyme function. In particular, direct kinetic measurements of individual steps occurring after enzymes adsorb to the cellulose surface have proven to be experimentally elusive. This work describes an experimental and analytical approach, derived from a detailed mechanistic model of cellobiohydrolase action, for determining rates of initial- and processive-cut product generation by *Trichoderma longibrachiatum* cellobiohydrolase I (*Tl*Cel7A) as it catalyzes the hydrolysis of bacterial microcrystalline cellulose (BMCC) alone and in the presence of *Talaromyces emersonii* endoglucanase II (*Tem*GH5). This analysis revealed that the rate of *Tl*Cel7A-catalyzed hydrolysis of crystalline cellulose is limited by the rate of enzyme complexation with glycan chains, which is shown to be equivalent to the rate of initial-cut product generation. This rate is enhanced in the presence of endoglucanase enzymes. The results confirm recent reports about the role of morphological obstacles in enzyme processivity and also provide the first direct evidence that processive length may be increased by the presence of companion enzymes, including small amounts of *Tem*GH5. The findings of this work indicate that efforts to improve cellobiohydrolase activity should focus on enhancing the enzyme's ability to complex with cellulose chains, and the analysis employed provides a new technique for investigating the mechanism by which companion enzymes influence cellobiohydrolase activity.
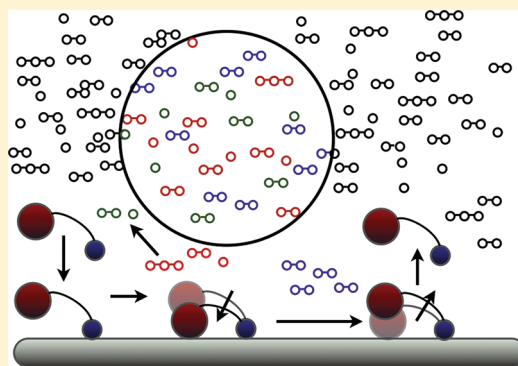
Cellobiohydrolases comprise a major class of cellulase enzymes, which catalyze the hydrolysis of insoluble cellulose into soluble sugars. In Nature, they are the largest single component of the multicellulase mixtures secreted by cellulolytic fungi;[1] in industry, they are a common target of enzyme engineering strategies that aim to develop more efficient saccharification systems for the production of cellulosic biofuels.[2] Efforts to understand and improve cellobiohydrolase activity in cellulolytic mixtures have been hindered by the experimental difficulties presented by the heterogeneous biocatalytic systems in which they participate.[3−5]

Once adsorbed to the cellulose surface, cellobiohydrolases participate in a series of reaction steps that are difficult to study in isolation.[6−8] Experimental evidence of a particular rate-limiting kinetic step has therefore remained elusive. In this work, we employed an experimental approach, based on a detailed mechanistic model of cellobiohydrolase action, to identify the rate limitations imposed upon *Trichoderma longibrachiatum* cellobiohydrolase I (*Tl*Cel7A) as it catalyzes the hydrolysis of bacterial microcrystalline cellulose (BMCC) alone and in the presence of *Talaromyces emersonii* endoglucanase II (*Tem*GH5).

Cellobiohydrolases (CBHs, EC 3.2.1.91) and endoglucanases (EGs, EC 3.2.1.4) represent the two broad cellulase classes. Both have active sites consisting of two glutamate and/or aspartate residues positioned to promote general acid-catalyzed hydrolysis of the β-1,4-bonds that link the repeating cellobiose subunits of cellulose chains.[9−11] The distance between these catalytic residues (5.5 or 10 Å) determines whether hydrolysis results in a retention or inversion of the anomeric carbon's configuration. In cellobiohydrolases, which hydrolyze cellulose processively from either the reducing or non-reducing chain end, the active site is located within a tunnel that can accommodate 6−10 glucosyl units.[12,13] In endoglucanases, which catalyze hydrolysis within cellulose chains, it is located within a 3−5-residue binding site cleft.[14] In both cases, the catalytic domain is linked via a 6−109-residue polypeptide linker to a smaller cellulose binding module (CBM), which facilitates adsorption to insoluble cellulosic substrates.[15] Endoglucanases sometimes lack a CBM, but cellobiohydrolases with such architectures have not been found.

The *Tl*Cel7A and *Tem*GH5 enzymes used in this study are thermostable examples of GH7 and GH5 cellulases. *Tl*Cel7A is a retaining cellobiohydrolase with a 10-residue binding site tunnel that facilitates processive hydrolysis from the reducing ends of cellulose chains.[12] *Tem*GH5, which has been less

extensively studied, is a retaining endoglucanase that appears to lack a CBM domain and binds cellulose with a binding site cleft that allows it to catalyze hydrolysis from a position within cellulose chains.[16,17]

Possible reaction paths used by these enzymes as they hydrolyze insoluble, heterogeneous cellulosic materials have been proposed in the literature (Figure 1).[3] (1) A cellobiohydrolase
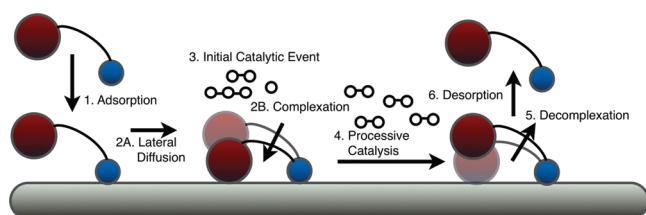

Figure 1. General conceptual picture of the reaction path used by cellobiohydrolases as they hydrolyze insoluble cellulose. Steps for strict endoglucanases are similar, but they do not engage in processive catalysis.

adsorbs to the crystalline regions of the cellulose surface via its CBM domain.[18−20] (2) It diffuses along the surface and forms complexes with a cellulose chain end via its catalytic domain.[21] (3) It catalyzes an initial hydrolysis event, generating glucose, cellobiose, or cellotriose (G_1, G_2, or G_3, respectively).[22−24] (4) It catalyzes subsequent hydrolysis events, generating only G_2, as it processively moves along the chain.[25,26] (5) It decomplexes from the cellulose chain.[27] (6) It recomplexes with a cellulose chain or desorbs from the surface. Endoglucanases undergo similar steps, but they are generally thought to engage in a nonprocessive random attack of less crystalline regions with single chains exposed. These enzymes generate both soluble and insoluble products, depending on the length of the polymer they are hydrolyzing and the position of the hydrolyzed glycosidic linkage being broken.

Over the past 30 years, numerous mechanistic models describing the kinetics of cellulase-catalyzed hydrolysis of cellulose have been developed to determine the rate limitations of enzymatic hydrolysis.[3,4,28−33] Often relying on simplified representations of cellulose (including those of a soluble polymer, a bulk phase substrate, a multicomponent mixture, or a periodic flat surface), these studies have been limited in their ability to determine kinetic limitations arising form the nature of the cellulose surface (surface diffusion, chain abstraction, processivity, and decomplexation).[29−31,33] Almost all of these studies conclude that more experimental insights into surface reactions are required. Experimental efforts have been made to measure the rates of steps 1, 4, and 5 for Cel7A; however, conclusions about the sensitivity of overall hydrolysis kinetics to these steps have been difficult to draw in the absence of rate data for steps 2 and 3.[25,27,34,35]

Initial- and processive-cut TlCel7A product profiles can be employed to reveal the kinetic limitations imposed by complexation of an adsorbed cellobiohydrolase with chain ends and by subsequent processive catalysis. When compared to initial rate measurements on soluble cello-oligosaccharide chain ends, initial-cut product profiles from crystalline hydrolysis can reveal kinetic impediments associated with adsorption and complexation. Together with initial-cut time courses, processive-cut profiles can reveal limitations associated with processivity.

Endoglucanase enzymes engage in complementary hydrolysis activities that reveal the limitations of initial and processive

modes of cellobiohydrolase catalysis. Endoglucanases increase the concentration of free chain ends on the substrate surface and, by acting preferentially on partially exposed cellulose chains, may decrease the amount of solution-exposed pseudoamorphous regions.[36] The response of initial- and processive-cut TlCel7A product profiles to the presence of increasing concentrations of endoglucanase enzymes can reveal not only the surface features that limit TlCel7A complexation and processivity but also the kinetic limitations imposed by them.

We used measurements of cello-oligosaccharide production from bacterial microcrystalline cellulose (BMCC) obtained with either (1) identical concentrations of TlCel7A and different concentrations of TemGH5 or (2) different concentrations of TlCel7A acting alone to calculate time course profiles for the rates of initial and processive cellobiohydrolase hydrolysis events. We show that initial-cut products are reporters of the complexation of adsorbed cellobiohydrolases with glycan chains and that ratios of processive- to initial-cut products at later times serve as a measure of processive length. Profiles of initial-cut products, processive-cut products, and the ratio of the two permit assessment of the extent to which the overall hydrolysis process is limited by the reaction steps associated with an adsorbed cellobiohydrolase's engagement with cellulose chain ends and by those associated with its subsequent processive hydrolysis. This represents the first experimental attempt to directly study (1) cellobiohydrolase complexation kinetics and their impact on overall rates of cellulose hydrolysis and (2) the influence of endoglucanase enzymes on cellobiohydrolase complexation kinetics and on processive length.

■ EXPERIMENTAL PROCEDURES

Enzyme Purification. Both T. longibrachiatum cellobiohydrolase I (TlCel7A) and Ta. emersonii EG2 (TemGH5) were purchased from Megazyme and purified to single-band purity as described in the Materials and Methods of the Supporting Information. A 5 h assay of each enzyme against 10 g/L carboxymethyl cellulose ensured TlCel7A purity. At 0.27 μM, TemGH5 hydrolyzed ∼50% of the substrate in 5 h, but TlCel7A had no detectable activity against it, indicating no endoglucanase contamination of TlCel7A (Materials and Methods of the Supporting Information).

Cellulose Preparation. Pretreatment effects were minimized in the preparation employed here by the exclusion of steps involving strongly acidic or basic solutions.

A 20 μL freezer stock of Acetobacter xylinum (ATCC 53582) was used to inoculate 1 L of medium as described previously.[37] This inoculum was grown in a 2 L Erlenmeyer flask for 7 days at 25 °C in a shaker at 250 rpm; the resulting cellulose was purified as described in the Materials and Methods of the Supporting Information. The final cellulose concentration was measured with the phenol sulfuric acid method.[37,38]

Measurement of the TlCel7A Initial-Cut Product Distribution. The first-cut product distribution generated by TlCel7A after it binds to cellohexaose was measured with initial rate experiments. Sugar production was monitored for 2 min in 100 μL reaction mixtures containing 0.01 μM TlCel7A, 1390 μM cellohexaose (G_6), and 50 mM sodium acetate buffer (pH 4.8). The G_6 solution (with buffer) was incubated for 5 min in a 96-well polymerase chain reaction plate at 50 °C before 4.2 μL of the enzyme was added to bring the total volume to 100 μL. Reactions were stopped at 0, 20, 40, 60, 80, 100, and 120 s with 100 μL of a 0.100 M NaOH solution. Concentrations of

glucose (G_1), cellobiose (G_2), cellotriose (G_3), cellotetraose (G_4), and cellopentaose (G_5) were measured with a Dionex ICS-3000 instrument equipped with a CarboPac PA200 column and a Dionex Electrochemical Cell detection unit. All reactions were conducted in triplicate.

Measurement of Cellotriose Hydrolysis Rates. The Michaelis–Menten kinetic parameters for the activity of *Tl*Cel7A and *Tem*GH5 on cellotriose were calculated with nonlinear regression of initial rate data (Datagraph, Figure S2A,B of the Supporting Information). Hydrolysis was monitored in 100 μL reaction mixtures with 0.051 μM *Tl*Cel7A or 0.074 μM *Tem*GH5 in 50 mM sodium acetate (pH 4.8) buffer (50 °C). Initial cellotriose concentrations of 10.13, 50.65, 202.6, 506.5, and 919.804 μM were used for *Tl*Cel7A and 7.61, 50.03, 194.25, 476.02, 865.07, and 3323.6 μM for *Tem*GH5. Reactions were stopped after 1, 2, 3, and 4 h with 100 μL of 0.10 M NaOH, and glucose production was measured on the Dionex high-performance liquid chromatography system.

Measurement of Cello-Oligosaccharide Production in Various Mixtures. Cello-oligosaccharide production by defined mixtures of *Tl*Cel7A and *Tem*GH5 acting on BMCC was monitored discretely over the course of 120 h. In humidified shakers at 50 °C (200 rpm), reactions were conducted in 250 mL Erlenmeyer flasks containing 25.25 mL of 1 g/L BMCC, 50 mM sodium acetate buffer (pH 4.8), 0.01% sodium azide, and enzyme concentrations as described in Table 1.

Table 1. Enzyme Loadings in Various Mixtures

reaction	[Cel7A] (μM)	[GH5] (μM)	reaction	[Cel7A] (μM)	[GH5] (μM)
1	0	0	3B	0.152	0
2A	0	0.022	3C	0.305	0
2B	0	0.037	4A	0.076	0
2C	0	0.19	4B	0.076	0.0187
2D	0	0.37	4C	0.076	0.0935
2E	0	0.74	4D	0.076	0.187
3A	0.015	0	4E	0.076	0.374

Samples were taken from reaction mixtures 1, 3A–3C, and 4A–4E at the following times: 0, 1.17, 2.22, 3.42, 4.6, 5.93, 7.8, 13.15, 16.42, 20.87, 37.47, 45, 59.63, 68.33, 75.6, 86.08, 97.73, 110.4, and 120.6 h. Samples were taken from reaction mixtures 2A–2C at the following times: 0, 1.75, 6.3, 16.5, 21.4, 26.9, 32.3, 49, 98.1, and 121.1 h. At all time points, two 20 μL aliquots were withdrawn individually frozen and diluted with 0.05 M NaOH before being run on a Dionex system. All reactions were conducted in duplicate.

Analysis of Kinetic Data. Prior to detailed kinetic analysis, measurements likely to be erroneous were detected with a MATLAB program written for this study. When a single measurement increased the standard error associated with an average of four measurements of the same phenomenon to >10%, that measurement was removed from the data analyzed. Of the total data set, 19 measurements were removed; these represented ~2% of the total measurements. Bias resulting from the removal of this small percentage of data is unlikely to affect the results of this work.

Derivation of Equations for η. The development of equations for η, the fraction of enzymes that are not directly engaged in hydrolyzing the insoluble substrate, is described in section 1 of the Supporting Information.

Development of Equations for f. Derivations of equations for f, the fraction of cellotriose generated by *Tem*GH5 within *Tem*GH5/*Tl*Cel7A mixtures, are detailed in section 2 of the Supporting Information.

■ RESULTS

Determination of *Tl*Cel7A Initial- and Processive-Cut Product Generation Rates. The differences in product distributions generated by cellobiohydrolases hydrolyzing cellulose processively and nonprocessively permit the experimental assessment of the kinetic limitations of binding to, processing along, and dissociating from cellulose chains. Upon forming a complex with a glycan chain, *Tl*Cel7A generates G_1, G_2, and G_3 in a fixed ratio. The rate of *Tl*Cel7A initial-cut product (icut product) formation can therefore be written in terms of the rate of generation of G_3 from chain ends:

$$\frac{\mathrm{d}[\text{icut product}]_{Tl\text{Cel7A}}}{\mathrm{d}t} = \left(\frac{\mathrm{d}[G_3]_{Tl\text{Cel7A icut}}}{\mathrm{d}t}\right)(1 + \alpha + \beta) \tag{1}$$

where

$$\alpha = \frac{\frac{\mathrm{d}[G_1]_{Tl\text{Cel7A icut}}}{\mathrm{d}t}}{\frac{\mathrm{d}[G_3]_{Tl\text{Cel7A icut}}}{\mathrm{d}t}}; \quad \beta = \frac{\frac{\mathrm{d}[G_2]_{Tl\text{Cel7A icut}}}{\mathrm{d}t}}{\frac{\mathrm{d}[G_3]_{Tl\text{Cel7A icut}}}{\mathrm{d}t}}$$

A material balance for G_3 can be used to express the right side of eq 1 in terms of measurable quantities. Both the initial cuts of *Tl*Cel7A and the "random attack" of *Tem*GH5 on BMCC generate G_3, and both enzymes can catalyze its hydrolysis. The following equation for G_3 production takes these processes into account:

$$\frac{\mathrm{d}[G_3]_{\text{observed}}}{\mathrm{d}t} = \frac{\mathrm{d}[G_3]_{Tl\text{Cel7A icut}}}{\mathrm{d}t} + \frac{\mathrm{d}[G_3]_{Tem\text{GH5BMCC}}}{\mathrm{d}t} - \frac{\mathrm{d}[G_3]_{G_{3\text{hyd}}}}{\mathrm{d}t} \tag{2}$$

Equations 1 and 2 can be combined to yield

$$\frac{\mathrm{d}[\text{icut product}]_{Tl\text{Cel7A}}}{\mathrm{d}t} = (1 + \alpha + \beta)\left(\frac{\mathrm{d}[G_3]_{\text{obs}}}{\mathrm{d}t} + \frac{\mathrm{d}[G_3]_{G_{3\text{hyd}}}}{\mathrm{d}t} - \frac{\mathrm{d}[G_3]_{Tem\text{GH5BMCC}}}{\mathrm{d}t}\right) \tag{3}$$

In eqs 2 and 3, soluble cello-oligosaccharide chains consisting of more than three glucosyl units are not considered as separate sources of G_3 production. While cellotetraose (G_4), cellopentaose (G_5), and cellohexaose (G_6) are slowly generated by the action of *Tem*GH5 on cellulose, they are quickly hydrolyzed by the same enzyme; thus, their production is included in the last term of either equation. Cello-oligosaccharide chains with more than six glucose subunits are insoluble.

While retaining glycosyl hydrolase enzymes have been shown to be capable of catalyzing transglycosylation, this activity has been measured to be minor in comparison with their hydrolytic activities by Harjunpaa et al.,[40] Gusakov et al.,[39] and Vřanská et

al.[24] Thus, as in kinetic models presented by Okazaki et al.,[29] Bezzera et al.,[42] Praestgaard et al.,[41] and Nidetzky et al.,[23] transglycosylation by *Tl*Cel7A and *Tem*GH5 was neglected in this analysis.

If the initial concentrations of all species are assumed to be zero, eq 3 can be integrated to obtain an expression for the concentration of initial-cut products that have been generated at any given time:

$$[\text{icutproduct}]_{Tl\text{Cel7A}}$$
$$= (1 + \alpha + \beta)([\text{G}_3]_{\text{obs}} + [\text{G}_3]_{\text{G}_{3\text{hyd}}}$$
$$- [\text{G}_3]_{Tem\text{EG2BMCC}}) \tag{4}$$

Each term on the right-hand side represents some discretely measurable or estimable quantity.

An expression for the concentration of processive-cut products at any given time can be derived in a fashion identical to that described above (eq 5):

$$[\text{pcut product}]_{Tl\text{Cel7A}}$$
$$= [\text{G}_2]_{\text{obs}} - [\text{G}_2]_{\text{G}_{3\text{hyd}}} - [\text{G}_2]_{Tem\text{GH5BMCC}}$$
$$- [\text{G}_2]_{Tl\text{Cel7A icuts}} \tag{5}$$

Measurement of Initial-Cut Product Distributions by *Tl*Cel7A on Chain Ends. The kinetic analysis employed here relies on previous reports that cellobiohydrolase enzymes generate glucose, cellobiose, and cellotriose as initial-cut products and that the initial-cut product distribution is the same for both soluble and solid substrates. The first assumption is supported well by the existing literature.[22−24,43] The second is based on a hypothesis that the factors influencing cellobiohydrolase product formation patterns result from substrate binding within the active site tunnel, rather than outside of it. Previous efforts to investigate processivity of cellobiohydrolases and chitinases suggest that initial-cut product distributions result from the tendency of the terminal glucosyl unit to occupy the +1, +2, and +3 sites located after the catalytic residues.[8,43] For *Trichoderma reesei* Cel7A, crystallographic data have revealed that the interaction between the enzyme and bound glycan is determined (1) by an extensive network of direct and indirect hydrogen bonds lining the entire tunnel and (2) by four tryptophan residues responsible for the −7, −4, −2, and +1 binding sites.[9,12] These data reveal an active site located seven binding sites into the enzyme, meaning that the dominant environment of a cello-oligosaccharide chain prior to being cleaved is the enzyme's interior. As the molecular determinants of binding are located inside the enzyme, the initial-cut product distribution that they influence should not depend on whether the substrate was soluble or abstracted from a surface. In this work, we have assumed this to be the case, and that substrate morphology is more likely to affect the rate at which initial cuts are generated and the rate with which chains are fed into the tunnel than the pattern of their cleavage once they get there. The limitations of this assumption are addressed below.

The initial-cut (G$_1$−G$_3$) product distribution for *Tl*Cel7A acting on insoluble substrate chain ends was determined from the initial rates of cellohexaose hydrolysis (G$_6$). A high cellohexaose concentration (∼100K_m), a low enzyme−substrate loading, and short reaction times were used to ensure that *Tl*Cel7A operated at a V_{max} corresponding to its rate of catalysis

at chain ends. Measured rates of G$_1$ and G$_2$ production were observed to be almost equivalent to the respective rates of G$_5$ and G$_4$ production (Table 2 and Figure S2 of the Supporting

Table 2. Kinetic Parameters

enzyme	substrate	parameter	value	source
*Tl*Cel7A	G$_6$	$(\text{d}[\text{G}_1]/\text{d}t)_i$	0.0142 μM/s	measured
*Tl*Cel7A	G$_6$	$(\text{d}[\text{G}_2]/\text{d}t)_i$	0.0038 μM/s	measured
*Tl*Cel7A	G$_6$	$(\text{d}[\text{G}_3]/\text{d}t)_i$	0.0118 μM/s	measured
*Tl*Cel7A	G$_6$	$(\text{d}[\text{G}_4]/\text{d}t)_i$	0.0033 μM/s	measured
*Tl*Cel7A	G$_6$	$(\text{d}[\text{G}_5]/\text{d}t)_i$	0.012 μM/s	measured
*Tl*Cel7A	G$_6$	$k_{\text{cat}Tl\text{Cel7A}}$	4.5 s^{-1}	measured
*Tl*Cel7A	G$_6$	$K_{MTl\text{Cel7A}}$	14.9 μM	measured
*Tl*Cel7A	G$_3$	$k_{\text{cat}Tl\text{Cel7A}}$	58.1 h^{-1}	measured
*Tl*Cel7A	G$_3$	$K_{MTl\text{Cel7A}}$	107.3 μM	measured
*Tl*Cel7A	G$_3$–G$_6$	K_{IG1}	10000 μM	3
*Tl*Cel7A	G$_3$–G$_6$	K_{IG2}	100 μM	31−33
*Tl*Cel7A	G$_6$	α	2.41	measured
*Tl*Cel7A	G$_6$	β	0.64	measured
*Tl*Cel7A	BMCC	ρ	2.7	estimated
*Tl*Cel7A	BMCC	K'_{eq}	0.592 μM	measured
*Tem*GH5	G$_3$	$k_{\text{cat}Tem\text{GH5}}$	910 h^{-1}	measured
*Tem*GH5	G$_3$	$K_{MTem\text{GH5}}$	960 μM	measured
*Tem*GH5	G$_3$–G$_6$	K_{IG1}	10000	3
*Tem*GH5	G$_3$–G$_6$	K_{IG2}	500	30
*Tem*GH5	BMCC	ρ	1	estimated
*Tem*GH5	BMCC	K'_{eq}	0.088 μM	measured

Information), suggesting that these products correspond only to initial cuts.[23,24]

Cellotriose Hydrolysis by *Tl*Cel7A and *Tem*GH5. Cellotriose hydrolysis by both enzymes was observed to follow Michaelis−Menten behavior modified to include competitive inhibition by G$_1$ and G$_2$ (Figure S2A,B of the Supporting Information):[44]

$$\frac{\text{d}[\text{G}_3]_{\text{hyd}}}{\text{d}t}$$
$$= \frac{-k_{\text{cat}Tl\text{Cel7A}}\eta_{Tl\text{Cel7A}}[Tl\text{Cel7A}]_{\text{total}}[\text{G}_3]}{[\text{G}_3] + K_{MTl\text{Cel7A}}\left(1 + \dfrac{[\text{G}_1]}{K_{\text{IG1}Cel7A}} + \dfrac{[\text{G}_2]}{K_{\text{IG2}Cel7A}}\right)} \tag{6}$$

$$\frac{\text{d}[\text{G}_3]_{\text{hyd}}}{\text{d}t} = \frac{-k_{\text{cat}Tem\text{GH5}}\eta_{Tem\text{GH5}}[Tem\text{GH5}]_{\text{total}}[\text{G}_3]}{[\text{G}_3] + K_{MTem\text{GH5}}\left(1 + \dfrac{[\text{G}_1]}{K_{\text{IG1}Tem\text{GH5}}} + \dfrac{[\text{G}_2]}{K_{\text{IG2}Tem\text{GH5}}}\right)} \tag{7}$$

where η_{CBH} and η_{EG} represent the fractions of each enzyme that are free to interact with soluble substrates (η = [enzyme free in solution or adsorbed to the cellulose but not complexed with cellulose chains]/[total enzyme]), i.e., uncomplexed with cellulose chains. Previous work has shown that such enzyme speciation exists.[3,27,45] All relevant kinetic constants from eqs 6 and 7 were measured from initial rate experiments or estimated from the literature[3,46−49] (Table 2).

Values of η_{CBH} and η_{EG} were estimated from constitutive equations based on three assumptions. (1) Cellulases can move to complexation sites only after becoming adsorbed to cellulose (complexation and adsorption are not coincident). (2) Cellulase adsorption and complexation are in equilibrium.[50] (3) The total enzyme concentration and total number of surface sites (adsorption sites and complexation sites) are assumed to be within 1 order of magnitude of each other.[27,34,51] An equation for η_{CBH} based on these assumptions takes the

form (Appendix and section 1 of the Supporting Information):

$$\eta_{TlCel7A} = \rho_{TlCel7A} \frac{[TlCel7A]_{total}}{K'_{eqTlCel7A} + [TlCel7A]_{total}} \quad (8)$$

where ρ_{CBH} is a proportionality constant that can be estimated from data provided by Kurasin et al.[27] and K'_{eqCBH} is the apparent equilibrium dissociation constant for complexed enzymes (Appendix and sections 1 and 2 of the Supporting Information). The equation for η_{EG} is identical in form. Values of ρ and K'_{eq} for each enzyme are included in Table 2.

For each mixture described in Table 1, rates of G_3 hydrolysis at 18 different time points were calculated from soluble cello-oligosaccharide measurements and the parameters described above using eqs 6 and 7 (Figure S3A of the Supporting Information). Fits to $d[G_3]_{G_{3hyd}}/dt$ versus t data were then integrated to yield time course profiles for G_3 hydrolysis (Figure S3B of the Supporting Information).

Estimation of Cellotriose Production by *Tem*GH5. Cellotriose resulting from the action of *Tem*GH5 on BMCC was estimated as a fraction f of the total G_3 produced in each reaction:

$$[G_3]_{TemGH5BMCC} = f([G_{3total}] + [G_{3hyd}]) \quad (9)$$

$$[G_2]_{TemGH5BMCC} = \lambda f([G_{3total}] + [G_{3hyd}]) \quad (10)$$

where

$$\lambda = \frac{[G_2]_{TemGH5BMCC}}{[G_3]_{TemGH5BMCC}}$$

In solutions containing *Tem*GH5 alone, λ did not vary significantly with time (Figure S4 of the Supporting Information). This observation is consistent with the "random attack" mechanism proposed for this enzyme, where it cleaves randomly within chains, generating soluble products either by cleaving near chain ends or by generating multiple cuts near the initial cut. Even if the degree of polymerization (DP) on the surface decreases throughout hydrolysis, a change in the pattern of glucose, cellobiose, or cellotriose generated from terminal glycosidic linkages is unlikely to result from a change in the number of such linkages on the surface. If these products are generated by multiple cuts close together, their ratio will also be independent of DP.

Values of f are difficult to measure, but upper and lower bounds can be estimated from eqs 11 and 12:

$$f(t) = \frac{\text{total } G_3 \text{ by } TemGH5 \text{ alone}}{\text{total } G_3 \text{ by } TemGH5 \text{ and } TlCel7A \text{ mix}}$$
$$= \frac{[G_3]_{totTemGH5i}}{[G_3]_{totalTemGH5i} + [G_3]_{totTlCel7Ai}} \quad (11)$$

$$f(t) = \frac{[G_3]_{\text{total by } TemEG2i}}{1.4([G_3]_{\text{total } TemGH5i} + [G_3]_{\text{total } TlCel7Ai})} \quad (12)$$

Equation 11 overestimates f by relying on an underestimate of the total amount of G_3 generated by a two-enzyme mixture (the denominator); *Tl*Cel7A and *Tem*GH5 are assumed to act in concert as they would in isolation (subscript i = isolation; Appendix and section 3A of the Supporting Information). Equation 12 underestimates f; in this equation, the concerted action of both enzymes is assumed to lead to an increase in G_3

production that is identical to the average increase in overall hydrolysis commonly reported when these enzymes are combined (Appendix and section 3B of the Supporting Information).[52] This increase is often described by the ratio defined by eq 13:

$$\frac{[G_{eq}]_{mix}}{[G_{eq}]_{TlCel7A} + [G_{eq}]_{TemGH5}} \quad (13)$$

where G_{eq} is the glucose equivalent of soluble products formed. In the reactions employed in this work, the average value of this ratio was 1.4 (Appendix and section 3C of the Supporting Information). Averages of upper and lower bounds of $f(t)$ were used to evaluate eqs 9 and 10 at each time point.

■ DISCUSSION

Complexation Limits Hydrolysis. The significance of rates of generation of initial-cut products from solid substrates can be explored through a comparison to rates on soluble substrates (Table 3). With 1.39 mM cellohexaose, a soluble

Table 3. Initial Rates of Initial-Cut Product Generation[a]

step	[substrate]	[GH5]	icut product rate [μM s^{-1} (μM TlCel7A)$^{-1}$]
icut on BMCC	1 g/L BMCC	0	0.015
icut on BMCC	1 g/L BMCC	0.019	0.021
icut on BMCC	1 g/L BMCC	0.094	0.044
icut on BMCC	1 g/L BMCC	0.187	0.093
icut on BMCC	1 g/L BMCC	0.374	0.108
icut on C_6	1.39 mM C_6	–	3.0

[a]Initial rates (averages of hydrolysis for the first 3 h) are normalized by TlCl7A concentration to facilitate comparison with the initial-cut experiments with TlCel7A on cellohexaose, where a lower concentration of enzyme had to be used to facilitate initial rate measurements. Rates reported here correspond to reactions 4A−4E in Table 1, where the TlCel7A concentration is held constant but the TemGH5 concentration is increased. These rates are 30−300 times slower than initial rates of initial-cut product generation on cellohexaose [3 μM s^{-1} (μM TlCel7A)$^{-1}$].

substrate, TlCel7A generated initial-cut products at a rate of 3 μM s^{-1} (μM TlCel7A)$^{-1}$. This cellohexaose concentration is ∼100 times the K_M of TlCel7A for this substrate; the rate observed, therefore, is dependent only on the enzyme concentration and the intrinsic rate of catalysis (k_{cat}). On 1 g/L BMCC, TlCel7A generated initial-cut products at initial rates of 0.01−0.1 μM s^{-1} (μM TlCel7A)$^{-1}$ (Table 3); these rates are 30−300 times slower than those on the soluble substrate. Unlike rates with cellohexaose as the substrate, however, the rates with insoluble substrates are not necessarily measured where [chain ends] $\gg K_{M-surface}$ (moles per surface area). To determine the maximal rates of hydrolysis where the chain end concentration was not limiting, TemGH5 endoglucanase was added to provide additional cellulose chain ends for TlCel7A action. In Table 3, the rate at which initial-cut TlCel7A products are generated from cellulose appears to reach a point at which it is independent of chain end surface concentration. The last two data points indicate that when the endoglucanase
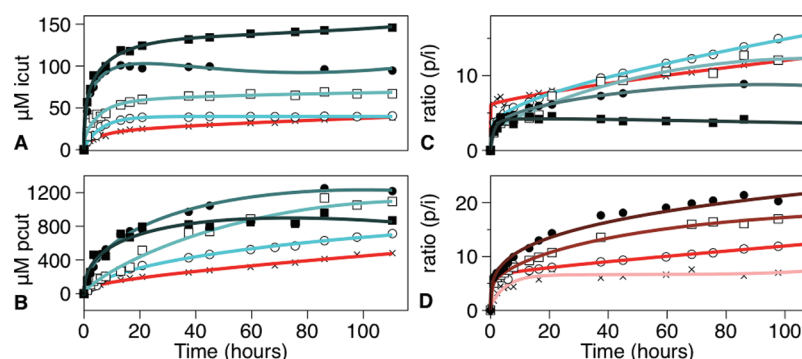
Figure 2. *Tl*Cel7A initial- and processive-cut product generation within various mixtures. For panels A−C, lines represent arbitrary fits for the following discretely measured quantities within each *Tl*Cel7A/*Tem*GH5 mixture (1 g/L BMCC, pH 4.85, 50 °C): (A) initial-cut products, (B) processive-cut products, and (C) the ratio between the two (p/i ratio = [pcut products]/[icut products]). The red line (×) corresponds to the mixture with 0.076 μM *Tl*Cel7A and no endoglucanase. All other mixtures have 0.076 μM *Tl*Cel7A and concentrations of *Tem*GH5 that are proportional to their shades of blue from lightest to darkest: 0.019, 0.09, 0.19, and 0.37 μM, respectively. For the reactions with *Tl*Cel7A alone, p/i ratio values are given in panel D. *Tl*Cel7A concentrations increase from light red to dark red: 0.0152, 0.076, 0.152, and 0.305 μM, respectively. Lines represent arbitrary fits to guide the eye.

concentration is doubled from 0.185 to 0.37 μM, the initial rate of initial-cut product generation by *Tl*Cel7A does not double, increasing instead from 0.093 to 0.107 μM s^{-1} (μM *Tl*Cel7A)$^{-1}$. While more endoglucase might enhance that rate, this small rate increase suggests that, in the presence of excess surface chains ([chain ends] ≫ K_M), the rate is no longer dependent on the availability of chain ends. The observed values on solid substrates, even with excess surface chains available, are still 1 order of magnitude lower than the analogous rate on soluble substrates.

Initial-cut products appear to be reporters for the complexation of *Tl*Cel7A enzymes with chain ends in the solid substrate. In accordance with the aforementioned rate disparities, the intrinsic rate of hydrolysis, which is at least as fast as the rate of generation of initial-cut products from soluble cello-oligosaccharides, does not govern the rate at which initial-cut products are formed from crystalline cellulose. Instead, the cellobiohydrolases seem to be impeded by the physical processes associated with their ability to adsorb to the substrate, diffuse along the cellulose surface, and form a complex with polymer chain ends. As adsorption has been shown to reach equilibrium within 1 h, the last two steps, termed complexation for this discussion, appear to determine the rate of initial-cut product formation.[53]

When compared with recently measured rates of *Trichoderma* Cel7A processivity, slow cellulose chain association rates appear to limit overall hydrolysis. In situ observations of *Tl*Cel7A cellobiohydrolases made with fast-scan AFM show processive speeds of ∼3.5 ± 1 nm/s.[25] This speed is approximately equal to the k_{cat} reported for this cellobiohydrolase multiplied by the length of a cellobiose unit (∼1 nm), and it amounts to a specific activity of ∼3.5 μM s^{-1} (μM processive *Tl*Cel7A)$^{-1}$ when cellobiose is the dominant product. Rates of processive catalysis measured by Igarashi et al. are nearly identical to the rates of generation of initial-cut products from soluble substrates measured here [3 μM s^{-1} (μM *Tl*Cel7A)$^{-1}$]; both appear to be governed by the intrinsic kinetics of the enzyme (k_{cat}). Thus, the kinetics of cellulose hydrolysis are primarily governed by the rates at which cellobiohydrolases become processive, not by the rates at which they process.

These results shed some light on the kinetic limitations imposed by the rate with which processive enzymes decomplex from cellulose chains. If enzymes that become "unstuck"

quickly re-engage in processive hydrolysis, then the rate at which they disengage with chain ends could limit overall hydrolysis kinetics. This argument has been made in the literature.[27] We find, however, that, early on, the ability of *Tl*Cel7A enzymes to initiate catalysis at chain ends is limited by the availability of those ends. Faster rates of decomplexation are only certain to increase rates of overall hydrolysis if complexation is fast, and we find that it is slow.

Surface Morphology Limits Processivity. The presence of additional physical and kinetic impediments to processive cellobiohydrolase action was evidenced in time course profiles showing the ratios of processive to initial cuts [p/i ratio (Figure 2C)]. The average number of processive events resulting from a single initial catalytic event is defined as the processive length (n_{pr}). For each cellulase mixture, the p/i ratio approaches a value of n_{pr} at later times. The p/i ratios at 110 h (∼n_{pr}) can be used as an estimate of processive length (Table 4); processive length values reported here

Table 4. Estimates of the Processive Length (n_{pr}) of Each Mixture^a

[Cel7A] (μM)	[GH5] (μM)	R (p/i)^b at 110 h (∼n_{pr})	X^c	[Cel7A] (μM)	[GH5] (μM)	R (p/i)^b at 110 h (∼n_{pr})	X^c
0.076	0	13	18	0.015	0	8	2
0.076	0.0187	16	26	0.076	0	13	32
0.076	0.0935	12	47	0.152	0	18	57
0.076	0.187	9	53	0.305	0	21	
0.076	0.374	4	60				

^{a}Estimates of processive length (n_{pr}) for each enzyme mixture. These estimates are based on the ratio of concentrations of processive-cut products to initial-cut products for a processive enzyme; this ratio levels off to the processive length of that enzyme. Figure 2 confirms this behavior. Values of processive length (n_{pr}) are estimated at 110 h (the 110 h time points from Figure 2). The dependence of processive length on the concentrations of *Tl*Cel7A and *Tem*GH5 enzymes is addressed in Discussion. ^{b}R (p/i) represents the p/i ratio. ^{c}X represents the percent conversion at 110 h.

are of the same order of magnitude as those reported in other studies of *Tl*Cel7A on BMCC.[27,54] As these values are 2 orders of magnitude lower than estimates of the intrinsic processive length of the *Trichoderma* Cel7A enzyme on this substrate (1000−4000), processive cellobiohydrolases are likely hindered by physical obstructions or decomplexation-encouraging surface features far

more frequently than they are stopped by the intrinsic kinetics of disengagement from cellulose chains. These findings are consistent with previous work showing that processive length depends on the nature of the substrate.[27]

These results also evidence the influence of endoglucanase enzymes on processive length (Table 4). Mixtures with 0.076 μM *Tl*Cel7A and 0.0187 μM *Tem*GH5 permit longer or equivalent processive lengths than the reaction with 0.076 μM *Tl*Cel7A alone. The failure of low *Tem*GH5 concentrations to reduce processive length by creating cuts in the surface is counterintuitive. By preferentially hydrolyzing exposed, pseudoamorphous cellulose chains on the cellulose surface, the regions upon which endoglucanases are most active, low concentrations of these enzymes may remove impediments, increasing the length over which processive cellobiohydrolase catalysis can occur. Other authors have provided evidence of the influence of surface morphology on cellobiohydrolase processive length, but our data provide evidence that morphological changes generated by low concentrations of endoglucanase enzymes may influence processive length.[27,45,55] The mechanism of these endoglucanase-influenced structural changes is not known.

At >0.0935 μM, *Tem*GH5 begins to restrict the processive length of *Tl*Cel7A (Figure 2C). This may result from a shortening of the average length of exposed cellulose strands or an enzyme crowding effect at the surface. As the latter has not previously been observed at the cellulase/cellulose loadings used in this study, the former is more likely.[3,56,57] At high concentrations, *Tem*GH5 may generate cuts within the crystalline regions to which *Tl*Cel7A binds, thus reducing the length over which *Tl*Cel7A can freely process. Mechanisms proposed here, however, are only speculative. In the end, the failure of low endoglucanase concentrations to rapidly decrease processive length deserves further experimental investigation.

Cellobiohydrolase Enzymes Potentiate Their Own Activity by Influencing Surface Morphology. In reactions with *Tl*Cel7A acting alone, the processive length increased with *Tl*Cel7A loading (Figure 2D and Table 4), suggesting that these enzymes may affect the morphology of the cellulose in a manner that increases its susceptibility to processive catalysis. Bacterial microcrystalline cellulose is predominantly in the I$_\alpha$ crystalline phase, which consists of cellulose chains aligned in parallel.[58] Previous work has shown that the *Tl*Cel7A cellobiohydrolase enzymes engage in unidirectional processive catalysis on the hydrophobic face of the crystal.[25,58,59] We speculate that cellobiohydrolases may be able to potentiate their own activity by clearing obstructions associated with imperfections in the packing of intertwined or closely aligned chains.

The change in processive length with cellobiohydrolase loading may also evidence the minor endo-like activity that has been reported for cellobiohydrolases.[27] This work reveals that small amounts of endoglucanase can increase processive length. The minor endo-like activity of cellobiohydrolase enzymes may function in a similar fashion; as the cellobiohydrolase concentration is increased, this endo-like activity, while still minor, may increase and lead to increased processive length in a manner similar to that of small amounts of endoglucanase. Previous work has shown that modification or removal of the four surface loops that form the active site tunnel of Cel7A can open its active site, increasing its endo-like character.[49,60] A processive- and initial-cut analysis similar to that used here but conducted with endo-like variants of Cel7A may reveal the

influence of endo activity on the ability of cellobiohydrolase enzymes to conduct processive catalysis.

Sensitivity of This Approach to Estimates Employed. These results showing that complexation is slow are unlikely to change if the initial-cut product distribution for *Tl*Cel7A is different on soluble and insoluble substrates. The product distribution is embedded in the $1 + \alpha + \beta$ coefficient of eq 3, which describes initial-cut products generated from insoluble cellulose. The $1 + \alpha + \beta$ term represents the total number of initial-cut products generated each time cellotriose is generated from an initial cut. For cellohexaose, the value of $1 + \alpha + \beta$ was found to be 4. Initial rates of initial-cut product generation on solid and soluble substrates were shown to differ by 1 order of magnitude when the initial-cut product distribution was assumed to be the same ($1 + \alpha + \beta = 4$) on solid and soluble substrates. For initial rates of initial-cut product generation to be equivalent on solid and soluble substrates, the value of $1 + \alpha + \beta$ would have to be ∼40 for cellulose. In such a case, the processive length corresponding to the reaction with 0.305 μM *Tl*Cel7A acting alone, the longest in this study, would be 2. This is 1 order of magnitude smaller than any processive length reported for this enzyme, indicating that a value of 40 for $1 + \alpha + \beta$ on solid cellulose is unrealistic.[27] Thus, even if initial-cut product distributions on solid and soluble substrates are different, they are unlikely to be sufficiently different to invalidate the result that complexation is rate-limiting.

The slow complexation result is similarly unaffected by the processive-cut product distribution. Previous studies have shown that cellobiose is the dominant product of processive catalysis.[22,23] In this work, cellobiose is treated as the only product of processive catalysis. If glucose and cellotriose are generated by processing cellobiohydrolase enzymes, the analysis employed within this work will lead to an overestimate for initial rates of generation of initial-cut products from soluble substrates. That is, they will be even slower than those reported in Table 4.

Processive length trends are insensitive to the initial-cut product distribution. The product distribution is incorporated in the $1 + \alpha + \beta$ coefficient in the $[G_2]_{TlCel7A \text{ icuts}}$ term of eq 5. Different initial-cut product distributions can increase or decrease the value of these terms, leading to higher or lower estimates of initial and processive cuts within all reactions. Processive length trends within and between reactions, however, are unaffected.

The qualitative trends illustrated by the initial- and processive-cut *Tl*Cel7A product profiles are insensitive to values of η and f (section 4 of the Supporting Information). Plots of eq 8 show that 10−90% of *Tem*GH5 or *Tl*Cel7A is available to hydrolyze soluble sugars at any given time, depending on the enzyme loading (Figure S4C,D of the Supporting Information). Values of ρ and K'_{eq} affect the value of η in any given mixture, but they do not affect the proportionality between η and the total enzyme concentration or the time-invariant nature of η. The trends illustrated in Figure 2 are most affected by these properties of η (section 4 of the Supporting Information), and thus, they are insensitive to the manner in which η is estimated. Estimates of f have a similar influence. The method employed to estimate f affects the *Tem*GH5 concentration at which further increases in *Tem*GH5 concentration lead to a reduction in processive length, rather than an increase, but this general trend, evident in Table 4, occurs with any f estimate (high, low, or average).

Enzyme Denaturation. The results of this work are not sensitive to the slow denaturation of the cellulase enzymes that were used. When grown on Avicel, *T. reesei* secretes a mixture

of cellulases that is dominated by Cel7A; the half-life of this mixture has been measured to be 43 h at 50 °C within a cellulose hydrolysis reaction mixture.[61] *Ta. emersonii* grows at higher temperatures than *T. reesei*, and many of its enzymes are more thermostable.[2] The half-life of *Tem*GH5 has not been explicitly measured, but we conservatively equate it to that of *Tl*Cel7A for the current discussion. Assuming an exponential model of decay, 95% of the enzymes will remain active in solution at 50 °C after 3 h, the period over which initial-cut product generation rates from insoluble cellulose were measured. This 5% inactivation of the enzyme is not enough to account for the initial-cut product generation rates being 3000−30000% slower on insoluble cellulose than on soluble cello-oligosaccharides.

Trends observed between the different reaction mixtures are similarly unaffected by enzyme denaturation. Each term in the kinetic equations used to calculate initial- and processive-cut products exhibits a first-order dependence on enzyme concentration. Reductions in enzyme concentration due to denaturation would affect both icut and pcut product concentrations in proportion to the concentration of enzyme present in each mixture; the trends observed between different reaction mixtures would remain unaffected.

Influence of Product Inhibition. The topic of product inhibition deserves special attention in our discussion of cellobiohydrolase kinetics. Glucose and cellobiose inhibition of cellobiohydrolase enzymes is well-known.[3,4,62] In a very recent study, Bu et al.[63] calculated the absolute free energies of binding of cellobiose to the Cel7A catalytic domain of *T. reesei* and found that this product is more stable in the enzyme tunnel than in free solution. The work of Bu et al. is significant in that it identifies the residues responsible for the enzyme's strong interaction with cellobiose, which acts as a competitive inhibitor and thereby reduces the effective enzyme concentration. If the level of inhibition by glucose and cellobiose is reduced, regardless of the rate-limiting step, rates of Cel7A-catalyzed cellulose hydrolysis will be increased.

Evidence of a Morphological Element to Enzyme Synergy. The sensitivity of cellobiohydrolase enzymes to the nature of the cellulose substrate may provide a rationale for the evolution of multienzyme mixtures produced by fungi. Cellulases are often grouped into two main classes (EG and CBH), but fungi such as *T. reesei* and *Neurospora crassa* produce multiple variants of each.[1,64] Several studies have demonstrated that carbohydrate-active enzymes have binding site preferences for different surface structures, which focus their activities onto proximal regions.[65,66] Such preferences may allow different cellulases to interact with and hydrolyze a wider variety of surfaces, thus relaxing the fidelity and sensitivities that might otherwise limit two-enzyme mixtures. Recent investigations into the role of GH61 enzymes, which are produced by *N. crassa* and other filamentous fungi, reinforce this hypothesis. This enzyme, which falls into neither cellulase class, has been shown to have a stimulatory effect on cellulases that likely results from an influence on surface morphology or an ability to oxidatively generate cuts within crystalline cellulose regions.[67,68]

Future Work with CBM-Containing Endoglucanase Enzymes. The results of this work are likely dependent on the morphological specificity of the enzymes used. The CBM-less *Tem*GH5 endoglucanase may have a more relaxed fidelity for particular surface structures than CBM-containing alternatives. There are 63 different families of CBM domains in the Carbohydrate Active Enzyme Database,[69] and different adsorption behaviors and cellulose morphology specificities have been observed among them.[70,71] Future work includes attaching CBMs with demonstrated specificities to the catalytic domain of *Tem*GH5 and assessing the different influence of these variants on cellobiohydrolase behavior. A crystalline-specific CBM may make the enzyme less likely to act on amorphous or paracrystalline cellulose, and therefore less effective in increasing the processive length of cellobiohydrolase enzymes. This is speculation, however, and the experiments still need to be performed.

■ CONCLUSIONS

Complexation has been previously assumed to be rate-limiting, and endoglucanases have been shown to influence complexation rates. This work provides direct experimental measurement of complexation rates to validate these assumptions. These results complement recently published MD simulations evidencing high energy barriers associated with glycan chain abstraction with kinetic measurements showing slow rates of cellobiohydrolase complexation, a process in which cellulose chain decrystallization is a key step.[63,72,73]

This study has several major implications for the design of better saccharification systems. First, cellobiohydrolase engineering efforts should focus on the development of enzymes with enhanced abilities to find and form complexes with chain ends. Results presented here show cellobiohydrolase complexation rates to be slow relative to those of other kinetic steps; enzymes that can more quickly extract chains from the cellulose surface are therefore likely to catalyze the hydrolysis of insoluble cellulose at higher rates. Second, this work presents the first experimental evidence that cellulases may remove the physical obstructions that cause cellobiohydrolases to become stuck. Endoglucanases are shown to potentiate the activity of cellobiohydrolases, not only by generating free chain ends but also by altering the surface in a way that increases that enzyme's processive length. Cellobiohydrolases are shown to potentiate their own activity in an identical processive length-enhancing fashion. Investigations that elucidate the mechanisms of these morphology-influenced enzyme synergies will facilitate the design of multicellulase mixtures. Such efforts would be complementary to recent studies showing that pretreatment-derived structural changes in the cellulose surface can make it more susceptible to cellobiohydrolase-catalyzed hydrolysis.[74,75] Ultimately, pretreatment methods, engineered cellulases, and novel helper enzymes (e.g., GH61 family enzymes) that facilitate the access of cellobiohydrolases to chain ends and reduce the incidence of surface obstructions will provide the most effective means of improving the rate and cost-effectiveness of the conversion of biomass to sugars.

■ ASSOCIATED CONTENT

Ⓢ Supporting Information

Derivation of equations for η, ρ, and f and also eqs 11 and 12, sensitivity of the results to η and f, figures showing equilibria between different states of the cellobiohydrolase, initial-cut products generated by *Tl*Cel7A on cellohexaose, Michaelis−Menten plots of enzyme activity on cellotriose, plots used to derive equations for η, time course profiles for cellotriose-normalized sugar concentrations in *Tem*GH5-catalyzed hydrolysis reactions, and *Tem*GH5-catalyzed hydrolysis of cellotriose during BMCC hydrolysis, and supporting information and methods pertaining to protein and cellulose preparation. This

material is available free of charge via the Internet at http://pubs.acs.org.

AUTHOR INFORMATION

Corresponding Author
*Department of Chemical and Biomolecular Engineering, 491 Tan Hall, University of California, Berkeley, CA 94720-1462. Telephone: (510) 642-1387. Fax: (510) 643-1228. E-mail: blanch@berkeley.edu (H.W.B.) or clark@berkeley.edu (D.S.C.).

ABBREVIATIONS
TemGH5, *Ta. emersonii* GH5 endoglucanase; TlCel7A, *T. longibrachiatum* cellobiohydrolase Cel7A; G_i, cello-oligosaccharide of length i.

REFERENCES
(1) Martinez, D., et al. (2008) Genome sequencing and analysis of the biomass-degrading fungus *Trichoderma reesei* (syn. *Hypocrea jecorina*) (vol. 26, pg 553, 2008). *Nat. Biotechnol.* 26, 1193.

(2) Voutilainen, S. P., Murray, P. G., Tuohy, M. G., and Koivula, A. (2010) Expression of *Talaromyces emersonii* cellobiohydrolase Cel7A in *Saccharomyces cerevisiae* and rational mutagenesis to improve its thermostability and activity. *Protein Eng., Des. Sel.* 23, 69−79.

(3) Levine, S. E., Fox, J. M., Blanch, H. W., and Clark, D. S. (2010) A Mechanistic Model of the Enzymatic Hydrolysis of Cellulose. *Biotechnol. Bioeng.* 107, 37−51.

(4) Zhang, Y. H. P., and Lynd, L. R. (2004) Toward an aggregated understanding of enzymatic hydrolysis of cellulose: Noncomplexed cellulase systems. *Biotechnol. Bioeng.* 88, 797−824.

(5) Himmel, M. E. (2007) Biomass recalcitrance: Engineering plants and enzymes for biofuels production (vol 315, pg 804, 2007). *Science* 316, 982.

(6) Ting, C. L., Makarov, D. E., and Wang, Z. G. (2009) A Kinetic Model for the Enzymatic Action of Cellulase. *J. Phys. Chem. B* 113, 4970−4977.

(7) Crowley, M. F., Uberbacher, E. C., Brooks, C. L. III, Walker, R. C., Nimlos, M. R., and Himmel, M. E. (2008) Developing improved MD codes for understanding processive cellulases. *J. Phys.: Conf. Ser.* 125, 1.

(8) Horn, S. J., Sikorski, P., Cederkvist, J. B., Vaaje-Kolstad, G., Sorlie, M., Synstad, B., Vriend, G., Varum, K. M., and Eijsink, V. G. H. (2006) Costs and benefits of processivity in enzymatic degradation of recalcitrant polysaccharides. *Proc. Natl. Acad. Sci. U.S.A.* 103, 18089−18094.

(9) Divne, C., Ståhlberg, J., Teeri, T. T., and Jones, T. A. (1998) High-resolution crystal structures reveal how a cellulose chain is bound in the 50 angstrom long tunnel of cellobiohydrolase I from *Trichoderma reesei*. *J. Mol. Biol.* 275, 309−325.

(10) Koivula, A., Ruohonen, L., Wohlfahrt, G., Reinikainen, T., Teeri, T. T., Piens, K., Claeyssens, M., Weber, M., Vasella, A., Becker, D., Sinnott, M. L., Zou, J. Y., Kleywegt, G. J., Szardenings, M., Ståhlberg, J., and Jones, T. A. (2002) The active site of cellobiohydrolase Cel6A from *Trichoderma reesei*: The roles of aspartic acids D221 and D175. *J. Am. Chem. Soc.* 124, 10015−10024.

(11) Pereira, J. H., Chen, Z. W., McAndrew, R. P., Sapra, R., Chhabra, S. R., Sale, K. L., Simmons, B. A., and Adams, P. D. (2010) Biochemical characterization and crystal structure of endoglucanase

Cel5A from the hyperthermophilic *Thermotoga maritima*. *J. Struct. Biol.* 172, 372−379.

(12) Divne, C., Ståhlberg, J., Reinikainen, T., Ruohonen, L., Pettersson, G., Knowles, J. K. C., Teeri, T. T., and Jones, T. A. (1994) The three-dimensional crystal structure of the catalytic core of cellobiohydrolase I from *Trichoderma reesei*. *Science* 265, 524−528.

(13) Rouvinen, J., Bergfors, T., Teeri, T., Knowles, J. K. C., and Jones, T. A. (1990) Three-dimensional structure of cellobiohydrolase II from *Trichoderma reesei*. *Science* 249, 380−386.

(14) Sulzenbacher, G., Shareck, F., Morosoli, R., Dupont, C., and Davies, G. J. (1997) The *Streptomyces lividans* family 12 endoglucanase: Construction of the catalytic core, expression, and X-ray structure at 1.75 Å resolution. *Biochemistry* 36, 16032−16039.

(15) Sonan, G. K., Receveur-Brechot, V., Duez, C., Aghajari, N., Czjzek, M., Haser, R., and Gerday, C. (2007) The linker region plays a key role in the adaptation to cold of the cellulase from an Antarctic bacterium. *Biochem. J.* 407, 293−302.

(16) Cellulase (endo-β-glucanase) from *Talaromyces emersonii* (lot 30602) (2007) Megazyme.

(17) Murray, P., Collins, C., and Tuohy, M. (2002) Q8WZDZ_TALEM. Uniprot.

(18) Lehtiö, J., Sugiyama, J., Gustavsson, M., Fransson, L., Linder, M., and Teeri, T. T. (2003) The binding specificity and affinity determinants of family 1 and family 3 cellulose binding modules. *Proc. Natl. Acad. Sci. U.S.A.* 100, 484−489.

(19) Din, N., Damude, H. G., Gilkes, N. R., Miller, R. C., Warren, R. A. J., and Kilburn, D. G. (1994) C-1-C-X Revisited: Intramolecular Synergism in a Cellulase. *Proc. Natl. Acad. Sci. U.S.A.* 91, 11383−11387.

(20) KlemanLeyer, K. M., Siika-aho, M., Teeri, T. T., and Kirk, T. K. (1996) The cellulases endoglucanase I and cellobiohydrolase II of *Trichoderma reesei* act synergistically to solubilize native cotton cellulose but not to decrease its molecular size. *Appl. Environ. Microbiol.* 62, 2883−2887.

(21) Jervis, E. J., Haynes, C. A., and Kilburn, D. G. (1997) Surface diffusion of cellulases and their isolated binding domains on cellulose. *J. Biol. Chem.* 272, 24016−24023.

(22) Vuong, T. V., and Wilson, D. B. (2009) Processivity, Synergism, and Substrate Specificity of *Thermobifida fusca* Cel6B. *Appl. Environ. Microbiol.* 75, 6655−6661.

(23) Nidetzky, B., Zachariae, W., Gercken, G., Hayn, M., and Steiner, W. (1994) Hydrolysis of Cello-oligosaccharides by *Trichoderma reesei* Cellobiohydrolases: Experimental Data and Kinetic Modeling. *Enzyme Microb. Technol.* 16, 43−52.

(24) Vřanská, M., and Biely, P. (1992) The Cellobiohydrolase-I from *Trichoderma reesei* Qm-9414: Action on Cello-Oligosaccharides. *Carbohydr. Res.* 227, 19−27.

(25) Igarashi, K., Koivula, A., Wada, M., Kimura, S., Penttilä, M., and Samejima, M. (2009) High Speed Atomic Force Microscopy Visualizes Processive Movement of *Trichoderma reesei* Cellobiohydrolase I on Crystalline Cellulose. *J. Biol. Chem.* 284, 36186−36190.

(26) Beckham, G. T., Matthews, J. F., Bomble, Y. J., Bu, L. T., Adney, W. S., Himmel, M. E., Nimlos, M. R., and Crowley, M. F. (2010) Identification of Amino Acids Responsible for Processivity in a Family 1 Carbohydrate-Binding Module from a Fungal Cellulase. *J. Phys. Chem. B* 114, 1447−1453.

(27) Kurasin, M., and Väljamäe, P. (2011) Processivity of Cellobiohydrolases Is Limited by the Substrate. *J. Biol. Chem.* 286, 169−177.

(28) Converse, A. O., and Optekar, J. D. (1993) A Synergistic Kinetics Model for Enzymatic Cellulose Hydrolysis Compared to Degree-of-Synergism Experimental Results. *Biotechnol. Bioeng.* 42, 145−148.

(29) Okazaki, M., and Mooyoung, M. (1978) Kinetics of Enzymatic Hydrolysis of Cellulose: Analytical Description of a Mechanistic Model. *Biotechnol. Bioeng.* 20, 637−663.

(30) Fan, L. T., Lee, Y. H., and Beardmore, D. H. (1980) Mechanism of the Enzymatic Hydrolysis of Cellulose: Effects of Major Structural

Features of Cellulose on Enzymatic Hydrolysis. *Biotechnol. Bioeng. 22*, 177−199.

(31) Fenske, J. J., Penner, M. H., and Bolte, J. P. (1999) A simple individual-based model of insoluble polysaccharide hydrolysis: The potential for autosynergism with dual-activity glycosidases. *J. Theor. Biol. 199*, 113−118.

(32) Väljamäe, P., Sild, V., Pettersson, G., and Johansson, G. (1998) The initial kinetics of hydrolysis by cellobiohydrolases I and II is consistent with a cellulose surface-erosion model. *Eur. J. Biochem. 253*, 469−475.

(33) Holtzapple, M. T., Caram, H. S., and Humphrey, A. E. (1984) The Hch-1 Model of Enzymatic Cellulose Hydrolysis. *Biotechnol. Bioeng. 26*, 775−780.

(34) Kim, D. W., Kim, T. S., Jeong, Y. K., and Lee, J. K. (1992) Adsorption Kinetics and Behaviors of Cellulase Components on Microcrystalline Cellulose. *J. Ferment. Bioeng. 73*, 461−466.

(35) Hong, J., Ye, X. H., and Zhang, Y. H. P. (2007) Quantitative determination of cellulose accessibility to cellulase based on adsorption of a nonhydrolytic fusion protein containing CBM and GFP with its applications. *Langmuir 23*, 12535−12540.

(36) Nidetzky, B., Steiner, W., and Claeyssens, M. (1994) Cellulose Hydrolysis by the Cellulases from *Trichoderma reesei*: Adsorptions of Two Cellobiohydrolases, Two Endocellulases and Their Core Proteins on Filter Paper and Their Relation to Hydrolysis. *Biochem. J. 303*, 817−823.

(37) Zaar, K. (1977) Biogenesis of Cellulose by *Acetobacter xylinum*. *Cytobiologie 16*, 1−15.

(38) Dubois, M., Gilles, K. A., Hamilton, J. K., Rebers, P. A., and Smith, F. (1956) Colorimetric Method for Determination of Sugars and Related Substances. *Anal. Chem. 28*, 350−356.

(39) Gusakov, A. V., Protas, O. V., Chernoglazov, V. M., Sinitsyn, A. P., Kovalysheva, G. V., Shpanchenko, O. V., and Ermolova, O. V. (1991) Transglycosylation activity of cellobiohydrolase I from *Trichoderma longibrachiatum* on synthetic and natural substrates. *Biochim. Biophys. Acta 1073*, 481−485.

(40) Harjunpaa, V., Helin, J., Koivula, A., Siika-aho, M., and Drakenberg, T. (1999) A comparative study of two retaining enzymes of *Trichoderma reesei*: Transglycosylation of oligosaccharides catalysed by the cellobiohydrolase I, Cel7A, and the *β*-mannanase, Man5A. *FEBS Lett. 443*, 149−153.

(41) Praestgaard, E., Elmerdahl, J., Murphy, L., Nymand, S., McFarland, K. C., Borch, K., and Westh, P. (2011) A kinetic model for the burst phase of processive cellulases. *FEBS J. 278*, 1547−1560.

(42) Bezerra, R. M., Dias, A. A., Fraga, I., and Pereira, A. N. (2011) Cellulose Hydrolysis by Cellobiohydrolase Cel7A Shows Mixed Hyperbolic Product Inhibition. *Appl. Biochem. Biotechnol. 165*, 178−189.

(43) Teeri, T. T., Koivula, A., Linder, M., Wohlfahrt, G., Divne, C., and Jones, T. A. (1998) *Trichoderma reesei* cellobiohydrolases: Why so efficient on crystalline cellulose? *Biochem. Soc. Trans. 26*, 173−178.

(44) Michaelis, L., and Menten, M. L. (1913) Kinetics of Invertase Action. *Biochem. Z. 49*, 333−369.

(45) Jalak, J., and Väljamäe, P. (2010) Mechanism of Initial Rapid Rate Retardation in Cellobiohydrolase Catalyzed Cellulose Hydrolysis. *Biotechnol. Bioeng. 106*, 871−883.

(46) Gruno, M., Väljamäe, P., Pettersson, G., and Johansson, G. (2004) Inhibition of the *Trichoderma reesei* cellulases by cellobiose is strongly dependent on the nature of the substrate. *Biotechnol. Bioeng. 86*, 503−511.

(47) Becker, D., Braet, C., Brumer, H., Claeyssens, M., Divne, C., Fagerström, B. R., Harris, M., Jones, T. A., Kleywegt, G. J., Koivula, A., Mahdi, S., Piens, K., Sinnott, M. L., Ståhlberg, J., Teeri, T. T., Underwood, M., and Wohlfahrt, G. (2001) Engineering of a glycosidase Family 7 cellobiohydrolase to more alkaline pH optimum: The pH behaviour of *Trichoderma reesei* CeI7A and its E223S/A224H/L225V/T226A/D262G mutant. *Biochem. J. 356*, 19−30.

(48) Voutilainen, S. P., Puranen, T., Siika-aho, M., Lappalainen, A., Alapuranen, M., Kallio, J., Hooman, S., Viikri, L., Vehmaanpera, J., and Koivula, A. (2008) Cloning, expression, and characterization of novel thermostable family 7 cellobiohydrolases. *Biotechnol. Bioeng. 101*, 515−528.

(49) von Ossowski, I., Ståhlberg, J., Koivula, A., Piens, K., Becker, D., Boer, H., Harle, R., Harris, M., Divne, C., Mahdi, S., Zhao, Y. X., Driguez, H., Claeyssens, M., Sinnott, M. L., and Teeri, T. T. (2003) Engineering the exo-loop of *Trichoderma reesei* cellobiohydrolase, Ce17A. A comparison with *Phanerochaete chrysosporium* Cel7D. *J. Mol. Biol. 333*, 817−829.

(50) Ooshima, H., Sakata, M., and Harano, Y. (1983) Adsorption of Cellulase from *Trichoderma viride* on Cellulose. *Biotechnol. Bioeng. 25*, 3103−3114.

(51) Ding, H. S., and Xu, F. (2004) Productive Cellulase Adsorption on Cellulose. *ACS Symp. Ser. 889*, 154−169.

(52) Hoshino, E., Shiroishi, M., Amano, Y., Nomura, M., and Kanda, T. (1997) Synergistic actions of exo-type cellulases in the hydrolysis of cellulose with different crystallinities. *J. Ferment. Bioeng. 84*, 300−306.

(53) Linder, M., and Teeri, T. T. (1996) The cellulose-binding domain of the major cellobiohydrolase of *Trichoderma reesei* exhibits true reversibility and a high exchange rate on crystalline cellulose. *Proc. Natl. Acad. Sci. U.S.A. 93*, 12251−12255.

(54) Kipper, K., Väljamäe, P., and Johansson, G. (2005) Processive action of cellobiohydrolase Cel7A from *Trichoderma reesei* is revealed as 'burst' kinetics on fluorescent polymeric model substrates. *Biochem. J. 385*, 527−535.

(55) Eriksson, T., Karlsson, J., and Tjerneld, F. (2002) A model explaining declining rate in hydrolysis of lignocellulose substrates with cellobiohydrolase I (Cel7A) and endoglucanase I (Cel7B) of *Trichoderma reesei*. *Appl. Biochem. Biotechnol. 101*, 41−60.

(56) Ståhlberg, J., Johansson, G., and Pettersson, G. (1991) A New Model for Enzymatic-Hydrolysis of Cellulose Based on the Two-Domain Structure of Cellobiohydrolase-I. *Bio/Technology 9*, 286−290.

(57) Xu, F., and Ding, H. S. (2007) A new kinetic model for heterogeneous (or spatially confined) enzymatic catalysis: Contributions from the fractal and jamming (overcrowding) effects. *Appl. Catal., A 317*, 70−81.

(58) Nishiyama, Y., Sugiyama, J., Chanzy, H., and Langan, P. (2003) Crystal structure and hydrogen bonding system in cellulose 1(α), from synchrotron X-ray and neutron fiber diffraction. *J. Am. Chem. Soc. 125*, 14300−14306.

(59) Liu, Y.-S., Baker, J. O., Zeng, Y., Himmel, M. E., Haas, T., and Ding, H. S. (2011) Cellobiohydrolase hydrolyzes crystalline cellulose on hydrophobic faces. *J. Biol. Chem. 286*, 11195−11201.

(60) Meinke, A., Damude, H. G., Tomme, P., Kwan, E., Kilburn, D. G., Miller, R. C. Jr., Warren, R. A., and Gilkes, N. R. (1995) Enhancement of the endo-β-1,4-glucanase activity of an exocellobiohydrolase by deletion of a surface loop. *J. Biol. Chem. 270*, 4383−4386.

(61) Drissen, R. E. T., Maas, R. H. W., Van Der Maarel, M. J. E. C., Kabel, M. A., Schols, H. A., Tramper, J., and Beeftink, H. H. (2007) A generic model for glucose production from various cellulose sources by a commercial cellulase complex. *Biocatal. Biotransform. 25*, 419−429.

(62) Holtzapple, M., Cognata, M., Shu, Y., and Hendrickson, C. (1990) Inhibition of *Trichoderma reesei* Cellulase by Sugars and Solvents. *Biotechnol. Bioeng. 36*, 275−287.

(63) Bu, L. T., Beckham, G. T., Shirts, M. R., Nimlos, M. R., Adney, W. S., Himmel, M. E., and Crowley, M. F. (2011) Probing Carbohydrate Product Expulsion from a Processive Cellulase with Multiple Absolute Binding Free Energy Methods. *J. Biol. Chem. 286*, 18161−18169.

(64) Tian, C. G., Beeson, W. T., Iavarone, A. T., Sun, J. P., Marletta, M. A., Cate, J. H. D., and Glass, N. L. (2009) Systems analysis of plant cell wall degradation by the model filamentous fungus *Neurospora crassa*. *Proc. Natl. Acad. Sci. U.S.A. 106*, 22157−22162.

(65) Carrard, G., Koivula, A., Soderlund, H., and Beguin, P. (2000) Cellulose-binding domains promote hydrolysis of different sites on crystalline cellulose. *Proc. Natl. Acad. Sci. U.S.A. 97*, 10342−10347.

(66) Herve, C., Rogowski, A., Blake, A. W., Marcus, S. E., Gilbert, H. J., and Knox, J. P. (2010) Carbohydrate-binding modules promote the

enzymatic deconstruction of intact plant cell walls by targeting and proximity effects. *Proc. Natl. Acad. Sci. U.S.A. 107*, 15293−15298.

(67) Harris, P. V., Welner, D., McFarland, K. C., Re, E., Navarro Poulsen, J. C., Brown, K., Salbo, R., Ding, H., Vlasenko, E., Merino, S., Xu, F., Cherry, J., Larsen, S., and Lo Leggio, L. (2010) Stimulation of lignocellulosic biomass hydrolysis by proteins of glycoside hydrolase family 61: Structure and function of a large, enigmatic family. *Biochemistry 49*, 3305−3316.

(68) Vaaje-Kolstad, G., Westereng, B., Horn, S. J., Liu, Z., Zhai, H., Sorlie, M., and Eijsink, V. G. (2010) An oxidative enzyme boosting the enzymatic conversion of recalcitrant polysaccharides. *Science 330*, 219−222.

(69) Carbohydrate-Binding Module Family Classification (2011) Carbohydrate-Active Enzyme Database.

(70) Boraston, A. B., Bolam, D. N., Gilbert, H. J., and Davies, G. J. (2004) Carbohydrate-binding modules: Fine-tuning polysaccharide recognition. *Biochem. J. 382*, 769−781.

(71) Boraston, A. B., Kwan, E., Chiu, P., Warren, R. A. J., and Kilburn, D. G. (2003) Recognition and hydrolysis of noncrystalline cellulose. *J. Biol. Chem. 278*, 6120−6127.

(72) Beckham, G. T., Matthews, J. F., Peters, B., Bomble, Y. J., Himmel, M. E., and Crowley, M. F. (2011) Molecular-Level Origins of Biomass Recalcitrance: Decrystallization Free Energies for Four Common Cellulose Polymorphs. *J. Phys. Chem. B 115*, 4118−4127.

(73) Zhong, L. H., Matthews, J. F., Hansen, P. I., Crowley, M. F., Cleary, J. M., Walker, R. C., Nimlos, M. R., Brooks, C. L., Adney, W. S., Himmel, M. E., and Brady, J. W. (2009) Computational simulations of the *Trichoderma reesei* cellobiohydrolase I acting on microcrystalline cellulose I β: The enzyme-substrate complex. *Carbohydr. Res. 344*, 1984−1992.

(74) Chundawat, S. P., Bellesia, G., Uppugundla, N., da Costa Sousa, L., Gao, D., Cheh, A. M., Agarwal, U. P., Bianchetti, C. M., Phillips, G. N. Jr., Langan, P., Balan, V., Gnanakaran, S., and Dale, B. E. (2011) Restructuring the crystalline cellulose hydrogen bond network enhances its depolymerization rate. *J. Am. Chem. Soc. 133*, 11163−11174.

(75) Sathitsuksanoh, N., Zhu, Z., Wi, S., and Zhang, Y. H. (2011) Cellulose solvent-based biomass pretreatment breaks highly ordered hydrogen bonds in cellulose fibers of switchgrass. *Biotechnol. Bioeng. 108*, 521−529.